ChemElectroChem

Research Article
doi.org/10.1002/celc.202400587

Chemistry Europe
European Chemical Societies Publishing

www.chemelectrochem.org

Influence of the Electrolyte pH on the Double Layer Capacitance of Polycrystalline Pt and Au Electrodes in Acidic Solutions

Kun-Ting Song[+],[a] Peter M. Schneider[+],[a] Ivo Grabovac,[a] Batyr Garlyyev,[a] Sebastian A. Watzele,[a] and Aliaksandr S. Bandarenka*[a, b]

A deeper understanding of electrified solid/liquid interfaces of polycrystalline materials is crucial for optimizing energy conversion and storage devices, such as fuel cells, electrolyzers, and supercapacitors. After more than a century of research, the double-layer capacitance (C_{DL}) has proven to be one of the few relatively easily experimentally accessible quantitative measures for characterizing such interfaces. However, despite their great importance, systematic C_{DL} measurements are still not frequently associated with other interfacial properties. This work investigates the effect of the electrolyte pH on the C_{DL} for polycrystalline platinum (Pt(pc)) and gold (Au(pc)) electrodes using cyclic voltammetry and impedance spectroscopy in acidic solutions with a pH ranging from 0 to 2 without adding any supporting electrolyte. Interestingly, under these conditions, the C_{DL} for the Pt(pc) electrode increases with increasing electrolyte pH, while the C_{DL} for the Au(pc) electrode shows the opposite trend. The increasing trend for Pt(pc) cannot be quantitatively described by the classical Stern model due to the stronger adsorption phenomenon on Pt surfaces. Moreover, positive linear trends with pH were found for the potentials of minimum C_{DL} values and the potentials of maximum entropy for both electrodes, which closely correlate with reaction activities. However, the transition potentials of the constant phase element exponent (an element commonly used to approximate the behavior of the double layer in experiments) are only observed for the Pt electrode due to the phase transitions within the hydrogen adsorption/desorption and double-layer regions. These findings pose an important step toward revealing the interplay between essential interfacial parameters, which is crucial for a complete understanding of the electrical double layer.

Introduction

The electrical double layer (EDL) is the fundamental part of electrochemical systems, as it is the region where the critical interfacial processes take place.[1–5] Understanding its structure is essential to advance the development of more efficient energy devices.[6,7] However, it is a complex system with many different parameters influencing it, such as temperature, applied electrode potential, electrode and electrolyte composition, and the interaction between these two phases, which need more detailed exploration. One should note that the existing EDL theory does not usually consider the electrode composition and surface structure effects. It also does not take into account the chemical nature of the electrolyte. The pH effect is a good example of cases outside the focus of the theory: the consequence is the absence of quantitative means to explain and predict the double-layer capacitance (C_{DL}) trends for almost all (if not all) solid electrodes.

For instance, experimental studies on the temperature effect for Pt electrodes have shown changes in the C_{DL} due to altered ion association in the electrolyte solution with temperature variations,[8,9] which is central subject to current theoretical investigations.[10] Furthermore, the electrode potential strongly influences the EDL structure by affecting the arrangement of ions and water dipoles near the electrified solid-liquid interface, influencing the electrochemical processes.[11,12] Clearly, the electrode material plays a significant role in influencing the EDL as it is directly in contact with the electrolyte, building the solid-liquid interface. Carbon materials (such as graphite, graphene, carbon nanotubes, activated porous carbon, etc.) and metal-based materials (such as Pt, Au, Pd, etc.) are among the most widely studied systems and give insights into the EDL characteristics.[13–18] In addition, studies of different single-crystal facets revealed that the surface structure of the electrode plays a crucial role in shaping the EDL.[19] Finally, the electrolyte is one of the most important aspects to consider when discussing solid-liquid interfaces. Several recent studies have focused on the influence of "spectator" ions on parameters like the double-layer capacitance.[20–22] It was reported that the C_{DL} depends

[a] K.-T. Song,[+] P. M. Schneider,[+] I. Grabovac, B. Garlyyev, S. A. Watzele, A. S. Bandarenka
Physik-Department ECS, Technische Universität München, James-Franck-Str. 1, D-85748 Garching, Germany
Tel. +49 (0) 89 289 12531
E-mail: bandarenka@ph.tum.de

[b] A. S. Bandarenka
Catalysis Research Center TUM, Ernst-Otto-Fischer-Straße 1, 85748 Garching bei München, Germany

[+] Kun-Ting Song and Peter M. Schneider contributed equally to this work.

Supporting information for this article is available on the WWW under https://doi.org/10.1002/celc.202400587

decisively on the hydration energy of the alkali metal cation type in the electrolyte.

Moreover, the electrolyte concentration, i.e., electrolyte pH, has also been studied to understand the solid/liquid interface better.[23,24] For the Pt(111) electrode, one of the most widely studied electrochemical systems, Rizo et al. found that the potential of zero free charge (PZFC), describing at which potential the electrode has no surface free charge, is independent of the electrolyte pH, while the potential of zero total charge (PZTC) changes and the C_{DL} increases with increasing pH for acidic solutions.[25] Ohja et al. discovered that the Gouy-Chapman capacitance minimum, necessary for the determination of double layer properties, such as the potential of zero charge (PZC), can only be found for specific pH values, for example, pH = 4 for a Pt(111) single crystal facet.[14] Furthermore, Goyal et al. investigated an Au(111)-aqueous electrolyte interface where they found that the constant phase element (CPE) exponent term n, used to describe the double layer frequency response, decreased with increasing pH (for alkaline conditions). In contrast, the C_{DL} increased, which could be attributed to the adsorption of electrolyte anions to the Au(111) surface.[26]

The potential of maximum entropy (PME), as an important EDL parameter describing the potential where the entropy of double-layer formation is highest, is crucial for determining energy barriers and efficient charge transfer through the interface during electrochemical reactions.[27,28] For different systems, such as Ir(111) and polycrystalline Au, a strong dependency of the PME on the electrolyte pH was found.[29,30] For both systems, the PME increased significantly with increasing pH. Furthermore, Zheng et al. showed the importance of interfacial properties, such as the electrolyte pH, in electrochemical systems by examining its influence on the hydrogen binding energy and, therefore, the increase of the hydrogen oxidation and evolution reaction activity of various platinum-group metals with decreasing pH values under acidic conditions.[31] All these different findings demonstrate the importance of detailed investigations of interfacial EDL parameters to understand, tune, and optimize the efficiency of electrochemical systems. Nevertheless, more experimental research needs to be conducted in which several parameters describing the electrical double layer are combined in one study to gain deeper insight into the underlying mechanisms.

Ding et al.[32] investigated the influence of solution pH ranging from 0 to 2 on the PME by using laser-induced current transient (LICT) for two commonly studied systems: polycrystalline platinum (Pt(pc)) and gold (Au(pc)) electrodes in perchloric acid ($HClO_4$) solutions. The results indicate that the PME vs. the reversible hydrogen electrode (RHE) scale for both Pt(pc) and Au(pc) electrodes increases linearly with increasing pH. Fundamentally, the PME correlates with the reaction activity, i.e., the closer the PME to the thermodynamic equilibrium potential of an electrocatalytic reaction is, the faster the respective reaction should be. To further explore the influence of pH on the interfacial properties within the EDL region, we used two electrochemical methods to assess the C_{DL} in this work. One of them is cyclic voltammetry. The C_{DL} can be roughly calculated by extracting the steady-state capacitive current from different scan rates within a potential window where no redox reactions occur during a cyclic voltammogram (CV).[33] Besides this widely applicable method, electrochemical impedance spectroscopy (EIS) is a more accurate and highly informative tool to investigate solid-liquid interfaces with different contributions of various electrochemical processes taking place simultaneously at the interface.[34]

In this work, the focus was put on Pt(pc) and Au(pc) electrodes since most of the technologically applied materials nowadays are of polycrystalline nature. However, in contrast to single crystal systems, only little research attention is paid to the EDL behavior of polycrystals due to the intrinsic complexity, especially in higher concentrated acidic solutions. A combination of measurement techniques was applied to investigate, compare, and correlate various EDL parameters. Cyclic voltammetry and EIS measurements were used to determine the C_{DL} at different pH. In addition, results from LICT experiments at different pH were adopted in this research to determine the PME as an essential parameter describing the solid-liquid interface. Finally, a correlation between the measured C_{DL}, the potential of minimum C_{DL}, and the PME was established to demonstrate a comprehensive overview of how the electrolyte pH influences electrochemical systems.

Experimental

A three-electrode setup was used for the electrochemical measurements. The working electrodes (WEs) included a Pt(pc) electrode (Ø = 5 mm, MaTeck, Germany) and an Au(pc) electrode (Ø = 12 mm, arrandee™, Germany). A mercury-mercurous sulfate electrode (MMS) (0.6 M K_2SO_4, SI Analytics, Germany) was used as the reference electrode (RE), while a platinum wire (99.9% purity, MaTeck, Germany) and a gold wire served as the counter electrode (CE) for their corresponding WE. All recorded potentials were converted to the RHE scale. The electrochemical measurements were conducted *via* a VSP-300 potentiostat (Bio-Logic, France) and EC-Lab software (v11.43). To compensate for measurement artifacts in the EIS measurements at high frequencies caused by the impedance of the RE, a shunt capacitor was placed between RE and CE.[35]

Before the measurements, the electrochemical cell and all glassware were cleaned with a 3:1 mixture of H_2SO_4 (96% H_2SO_4, p.a., ISO, Carl Roth, Germany) and H_2O_2 (30% H_2O_2, p.a., ISO, Carl Roth, Germany). Then, they were rinsed several times alternately with boiling and cold ultrapure water (18.2 MΩcm, Merck Millipore, USA). To investigate the pH effect in an acidic environment, equivalent amounts of perchloric acid (70% $HClO_4$, Suprapur, Merck, Germany) were diluted with ultrapure water until the desired pH values were reached. Before every set of measurements, the cell and all attached parts were cleaned several times with hot ultrapure water. Freshly prepared electrolyte solutions were used to avoid contamination. The electrolyte was purged with Ar (5.0, Westfalen, Germany) for 30 minutes before each measurement to exclude O_2 and undesired side reactions. Subsequently, the Pt and Au electrodes were put into the Ar-saturated $HClO_4$ by a hanging meniscus configuration to ensure a well-defined surface area in contact with the electrolyte. Each electrochemical measurement began with a CV performed in the range of 0.08 V to 1.20 V vs. RHE and 0.08 V to 1.65 V vs. RHE for Pt(pc) and Au(pc) electrodes,

respectively, at a scan rate of 50 mV s^{-1} until a stable CV was achieved. All recorded CVs are corrected by iR compensation.

For the EIS measurements, a frequency range of 100 kHz to 1 Hz and 10 kHz to 1 Hz was employed for the Pt(pc) and Au(pc) electrodes, respectively. The potential window was set from 0.3 V to 0.6 V vs. RHE for the Pt(pc) electrode and from 0.04 V to 0.52 V vs. RHE for the Au(pc) electrode, with measurements taken in 20 mV increments using a 10 mV perturbation amplitude. The measurements were performed for $HClO_4$ concentrations equivalent to pH values of 0 to 2 in 0.5-unit intervals. The measurements were repeated at least three times for each pH to verify the results. The impedance data were analyzed via the EIS Spectrum Analyzer software[36] and assessed by Kramers-Kronig check procedures.

Results and Discussions

First, we investigated the EDL using cyclic voltammetry, as this presents a simple and fast method. Figure 1 shows the typical CVs of the Pt(pc) electrode in Ar-saturated $HClO_4$ solutions with pH values ranging from 0 to 2. The CVs represent three distinct regimes, including hydrogen desorption (and hydroxyl adsorption at defects), EDL region, and surface oxide formation during the anodic scan, and the reversed features during the cathodic scan. It is observed that the peaks within the hydrogen adsorption/desorption region, mainly attributed to (110) and (100) facets,[37–39] shift to a more positive potential with increasing pH. This behavior deviates from the thermodynamic expectation that redox peaks remain aligned at the same potential referenced to the RHE scale. Beyond the expected Nernstian shift due to electrolyte concentration effects, the peak shifts can be correlated to the additional competition and coadsorption of hydroxide and water molecules within the hydrogen adsorption region, which affects the hydrogen binding energies and alters the interface structures.[39–41] This pH dependency of the hydrogen adsorption peaks has been observed on step-site Pt electrodes, such as Pt(553).[42] Another possible explanation is related to the local variations in H^+ concentration, which affect the ionic strength of molecules and alter the electrochemical conditions.[43,44] A similar trend is observed in the potential region of surface oxide formation/reduction, where the peaks shift with increasing pH values. Furthermore, the solution pH also impacts the capacitive currents within the EDL region (see the inset of Figure 1). The "zoomed-in" view of the normalized capacitive current density increases with higher pH values. The pH dependence of the double-layer capacitance (C_{DL}) trend is consistent with literature studies for Pt electrodes,[14,45] but to a certain extent in some conflicts with the Stern model, which predicts the C_{DL} to decrease as solution ion concentration decreases in diluted systems.[46]

For comparison, Figure 2 and Figure S1 show the CVs for the Au(pc) electrodes in Ar-saturated $HClO_4$ electrolytes with the same pH range. Notably, the hydrogen underpotential deposition (HUPD) phenomenon is not prominent for Au(pc) electrodes, with the CVs primarily displaying two distinct features: the double layer region and the surface oxidation/reduction processes.[47] The redox peaks shift positively as the pH increases; however, the C_{DL} trend of Au(pc) shows the opposite trend compared to Pt(pc) and follows the classical model, which considers the absence of ion adsorption and predicts that a higher electrolyte concentration leads to a higher C_{DL}.[14,28,49] This behavior is attributed to the weaker ion/solvent interactions on Au surfaces compared to Pt,[50] leading to ionic concentrations being more dominant in the EDL region.

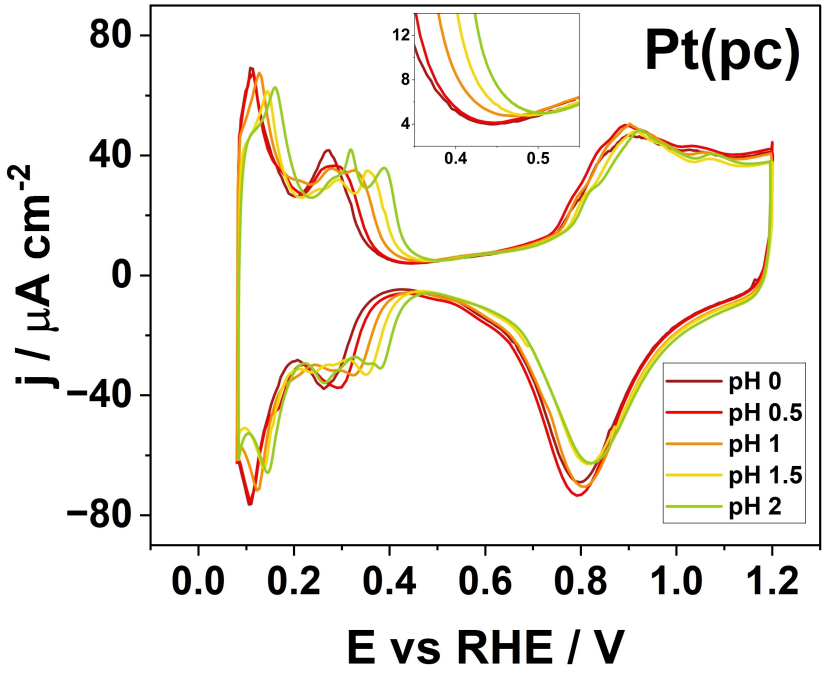

Figure 1. Typical CVs of the Pt(pc) electrode in Ar-saturated $HClO_4$ at different pH values (0, 0.5, 1, 1.5, and 2) at a scan rate of 50 mV s^{-1}. Three distinct regions can be observed, i.e., hydrogen adsorption/desorption (with corresponding OH-adsorption/desorption), double layer, and surface oxide formation/reduction.

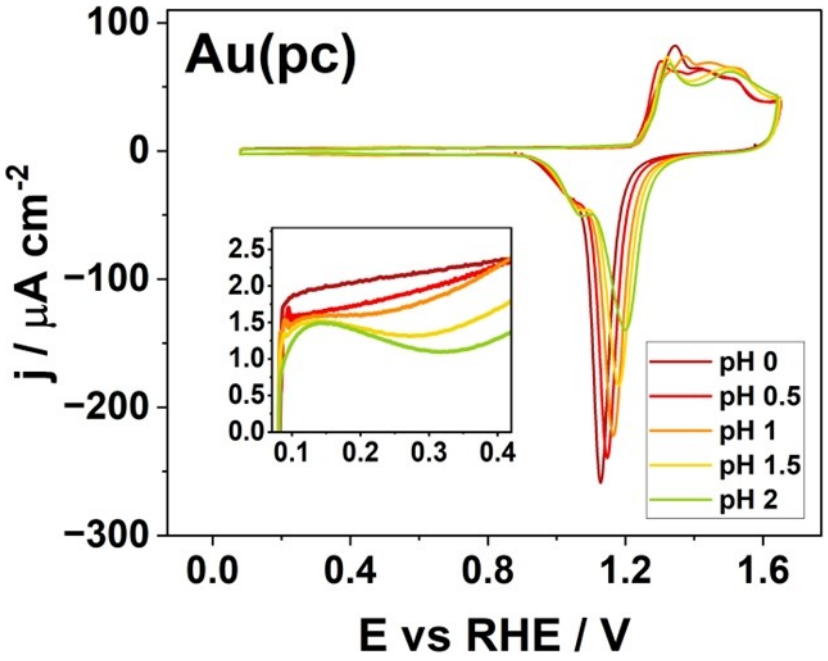

Figure 2. Typical CVs of the Au(pc) electrode in Ar-saturated $HClO_4$ at different pH values (0, 0.5, 1, 1.5, and 2) at a scan rate of 50 mV s^{-1}. Two distinct regions can be observed, i.e., double layer and surface oxide formation/reduction. The inset figure represents the magnification of current densities in the EDL region.

Furthermore, strongly adsorbed species, like HUPD and anion adsorptions, within the EDL region for Pt(pc) electrodes, could serve as a possible explanation for the different C_{DL} trends. As shown in Figure S1, the minimum double-layer capacitance ($C_{DL,min}$, denoted as data converted from current density divided by scan rate in Figure 1) is highly correlated with the estimated hydrogen adsorption charges, following the same linear increase with pH.

Besides, the Parsons-Zobel (PZ) plot provides an effective approach for examining the linear relationship between overall capacitance and diffuse-layer capacitance. Ohja et al. reported that the PZ slopes for Pt(111) and Au(111) electrodes in diluted solutions (pH = 4) are significantly lower than that of the Hg electrode, which shows a slope close to one and suggests minimal adsorption processes within the inner Helmholtz layer.[14] The smaller slope for Pt(111) compared to Au(111) further supports the notion that Pt(111) exhibits stronger ion interactions at the electrode/electrolyte interface. However, in this study, the observed opposite trend of C_{DL} for Pt(pc) electrodes in highly concentrated solutions (pH = 0–2) cannot be explained by PZ analysis. This discrepancy may be attributed to the presence of strongly chemisorbed ions on Pt surfaces. Additionally, the adsorbed ions may be partially charged rather than fully electroneutral, resulting in the difficulty of extracting the pure C_{DL}.[51] Another possible reason is that the polycrystalline electrodes studied herein are comprised of different crystal orientations with grain boundaries in between that could lead to an altered electrochemical response due to different contributions from different crystal facets.

Importantly, while cyclic voltammetry can offer insight into the effect of solution concentration on ion adsorption/desorption and the C_{DL}, it is not sufficient for accurately determining the C_{DL}. The influence of the selected potential range, adsorbed species, and non-linearity between capacitive current and scan rate contribute to this limitation.[52,53] For instance, it is difficult to determine the potential of minimum C_{DL} from the CVs of Au(pc) compared to the EIS method in more concentrated solutions within the same potential region (see Figure 2 and Figure 3B, respectively). Therefore, this work also employs the EIS method, which provides a more effective way of determining the C_{DL}. This technique can distinguish between the contribution of the fast behavior of the C_{DL} and slower adsorption processes based on different time constants,[9,54] allowing for a more detailed examination of interfacial properties, which is further discussed.

Figure 3 shows the EIS fitting results from the double-layer measurements for Pt(pc) and Au(pc) electrodes. The equivalent electric circuit (EEC) models shown in Figure S2 are utilized to analyze the EIS data.[9,20,21] These models incorporate an uncompensated resistance (R_U), which arises from the electrolyte's resistance and the experimental setup's electronic resistance. The impedance of the double layer (Z_{DL}) is modeled as a constant phase element (CPE), with $Z_{DL} = C'_{DL}{}^{-1}(j\omega)^{-n}$, where C'_{DL} is proportional to the double-layer capacitance, n is the CPE exponent, j is the imaginary unit, and ω is the angular frequency. As the n value is close to 1 ($n > 0.9$ in this work, see Figure S4), we consider C'_{DL} to be an ideal capacitance as the first approximation.[19] The ion adsorption processes (mainly proton and anion adsorptions) contribute to the resistance (R_{AD}) and capacitance (C_{AD}), which are parallel to Z_{DL}. The charge transfer resistance (R_{CT}) is included to account for possible

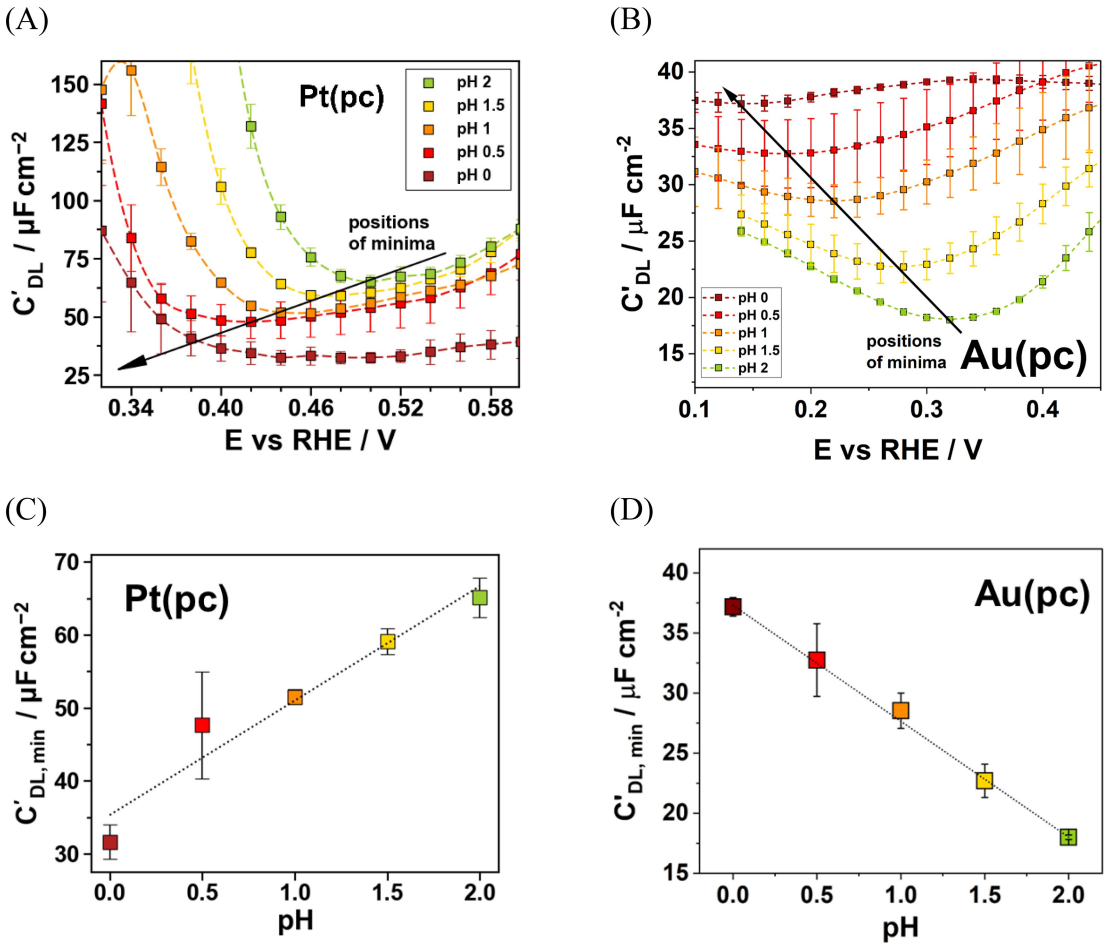

Figure 3. The C'_{DL} curves as a function of potential with the arrow indicating the trend of the potential of the $C'_{DL,min}$ for (A) Pt(pc) and (B) Au(pc) electrodes. $C'_{DL,min}$ as a function of the pH for (C) Pt(pc) and (D) Au(pc) electrodes extracted from (A) and (B), respectively. The dashed lines in (A) and (B) and the dotted lines in (C) and (D) illustrate a guide for the eye and the linear fitting, respectively.

Faradaic reactions from the residuals of oxygen in the measured system.

The fitting results for Pt(pc) and Au(pc) are shown in Figures 3A and B, respectively, as C'_{DL} curves versus RHE potential, as well as the trend of the potential of the minimum double-layer capacitance ($C'_{DL,min}$). The C'_{DL} trends observed for both electrodes using the EIS method are consistent with those observed in cyclic voltammetry (see Figures 1 and 2). However, the capacitances estimated from the EIS method in Figures 3C and D are lower than those obtained from the CVs. This discrepancy is further supported by the Nyquist impedance spectra (see Figure S4 and Figure S5), which do not exhibit a typical capacitive behavior characterized by a straight line. Instead, even at potentials within the double-layer region, the Nyquist plots exhibit a small semicircle and a tilted line from high to low frequencies, indicating the presence of slower ion adsorption processes compared to the faster responding speed of C'_{DL} at the electrode/electrolyte interface. Besides, the simplified EEC model (Figure S3), which includes only R_U and CPE elements and assumedly excludes any adsorption behaviors, is also employed to fit the impedance spectra for Au(pc) electrodes. Nevertheless, the $C'_{DL,min}$ fitting curves are more distinct when using a typical EEC model that accounts for the adsorption phenomena at the electrode/electrolyte interfaces. Furthermore, the values of $C'_{DL,min}$ for Pt(pc) are higher than those for Au(pc) at the same pH, suggesting a stronger metal/water interface for Pt(pc) characterized by a more condensed charge distribution compared to Au(pc).[48]

Notably, the C'_{DL} curves become smoother as the pH decreases for both electrodes, indicating that the Helmholtz capacitance, which remains approximately constant, becomes more dominant at higher concentrations.[14] Another crucial point is that surface geometry can significantly influence the kinetics of ion and solvent adsorption, particularly for Pt electrodes with stronger ion-surface interactions. For example, it has been reported that HUPD kinetics are slower on Pt(100) and Pt(311) surfaces compared to Pt(111) and Pt(110) surfaces,[55] leading to distinct CV profiles. The faster adsorption of hydrogen and hydroxyl species on the Pt(111) surface in acidic media can make it challenging to clearly distinguish C_{DL} from the adsorption-induced capacitance in the high-frequency regions. For example, the (111) facet on Pt exhibits a strong interaction with water molecules and the electrolyte that does not follow the mean-field Poisson-Boltzmann distribution,

leading to a Gouy-Chapman capacitance minimum only observable for more diluted electrolyte concentrations (near pH 4).[14] Since Pt(pc) electrodes combine various surface geometries, containing different crystal facets, lattice defects, and diverse grain structures, the EDL behavior might deviate strongly from its single crystal counterparts, hence the potentials of ion chemisorption may overlap with their C_{DL} behavior, resulting in a pseudo-capacitance effect. Due to the inherent difficulties in studying EDL systems in highly concentrated solutions, which are nonetheless more applicable to commercial energy conversion devices, it is recommended that further investigations of these complex physicochemical interfacial properties under varying ionic strengths of electrolytes are conducted using, for example, scanning probe techniques and simulation models that extend beyond the classical Stern model.[40,56,57]

Besides the influence of ionic concentration on C'_{DL} in acidic solutions, the CPE exponent, illustrating the capacitance frequency dispersion of the C_{DL}, provides additional information on the interfacial dynamics and surface structure for Pt and Au electrodes and depends on the applied potential in EIS.[58,59] Figures 4A and B show the comprehensive overview of CVs from Figures 1 and 2, including the EIS fitting results of the CPE exponent for Pt(pc) and Au(pc) electrodes from pH 0 to 2. Different hypotheses are trying to explain the origin of the CPE exponent behavior, which includes surface roughness, impurities, low electrolyte concentrations, nonuniform current distribution, etc.[15,56,60–62] Here, we illustrate the fraction of dissipation energy ($Diss_{CPE}$) of the ac probing signal in one harmonic cycle as another factor influencing the CPE exponent, as described by the following equation:[58,59]

$$Diss_{CPE}(\%) = \boldsymbol{cos}\left(\frac{n\pi}{2}\right)^{*} 100\% \quad (1)$$

where the n value is impacted by the degree of order of molecular arrangement on the local surface. Most n values within the measured potential region in this work are close to 1, which indicates that the surface has a structured double layer with less dissipation of energy. However, it is observed that there is a sharp peak drop of the CPE exponent for Pt(pc), including its minimum between the potential of the double-layer region and the onset potential of hydrogen adsorption/desorption (see Figure 4A for pH 1 and Figure S6). Consequently, this sharp decrease in the CPE exponent results in a higher energy loss involving higher frequency dispersion of the C_{DL}. This can be attributed to the 2D phase transition connected to the specific adsorption and additional solvent restructuring near the surface with hydrogen bond breaking [56]. As more ordered absorbate structures occur near the surface at the onset potential of proton adsorption/desorption, the ac probing

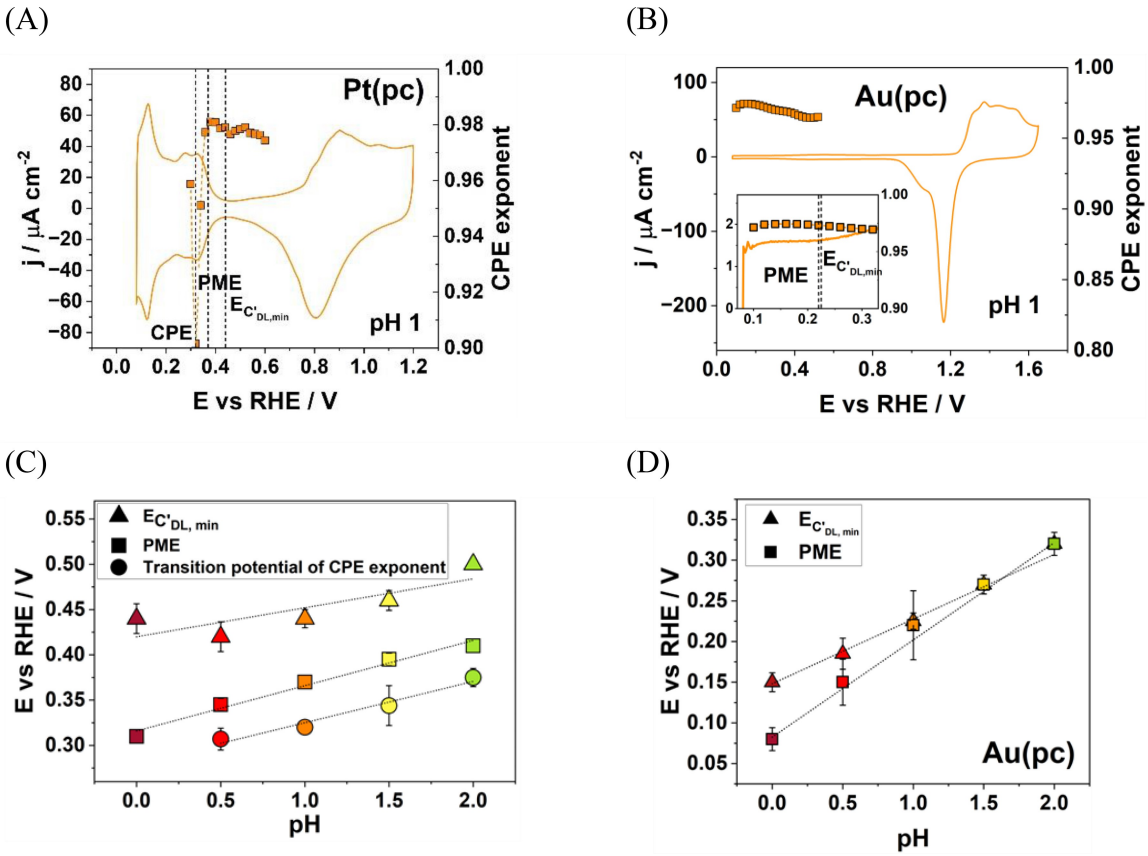

Figure 4. An overview of CVs for (A) Pt(pc) and (B) Au(pc) electrodes (obtained from Figure 1 and Figure 2) at a scan rate of 50 $mV\,s^{-1}$ with the fitting results of the CPE exponent versus the potential for pH 1. The figures include the positions of the potential of minimum C'_{DL} (denoted as $E_{C'DL,min}$) from Figures 3(A) and (B), PME, and the transition potential of the CPE exponent (denoted as CPE, only for Pt(pc)). The summarized parameters for (C) Pt(pc) and (D) Au(pc) in dependence on the electrolyte pH. The PME data are taken from reference.[32]

signal towards the interfacial double layer is influenced by the CPE exponent drop and has a higher energy dissipation. Conversely, the absence of a peak drop and the CPE exponent remaining close to 1 for Au(pc) electrodes across the measured pH values (see Figure 4B and Figure S7) can be explained by the weak HUPD process, suggesting no significant phase transition occurring within the potentials of the double-layer region.

For a better overview, the positions of the potential of $C'_{DL,min}$, the PME, and the order/disorder transition potential, where the CPE exponent has its minimum, are illustrated in dependence of the pH for Pt(pc) and Au(pc) electrodes in Figures 4C and D, respectively. It is noted that the PME data are taken from reference.[32] The difficulty of defining the transition potential of the CPE exponent at pH = 0 results in its exclusion. Interestingly, the potential of $C'_{DL,min}$, denoted as $E_{C'DL,min}$, which is close to the PZC, is located more positively compared to the PME. The results in this work for Pt(pc) are consistent with previous studies of Pt single crystals, which showed that the PZTC coincides nicely with the PME for Pt(111), while it is slightly more positive for Pt(100) and Pt(110) due to compensation with hydrogen adsorption charge.[63] As the Pt(pc) electrode comprises different crystal faces, as seen in the CVs in Figure 1, it is challenging to attribute the positive potential shift to a specific surface orientation. Müller et al. developed a model to simulate the capacitance response of a polycrystalline electrode for different electrolyte concentrations.[64] They showed that the differential capacity curves for a polycrystal deviate strongly from that of the different single-crystal facets and need to be derived from a mixed contribution of all present crystal orientations. Strikingly, the location of the capacitance minimum might not necessarily coincide with the PZC anymore, and the interpretation of the capacitance response is no longer intuitive, especially when considering adsorption or pseudocapacitive processes. Therefore, it can be assumed that the deviations of this work's C_{DL} and $E_{C'DL,min}$ results from those in single crystal studies in the literature depend strongly on the state of the polycrystalline electrodes' surface heterogeneity. Furthermore, the PME for each measured pH is located on the onset of the decrease of the CPE exponent fitting curve and is between $E_{C'DL,min}$, and the transition potential of the CPE exponent. This indicates that the PME, representing the maximum disorder of the water layer without specific adsorption at the solid/liquid interface, is slightly more positive compared to the transition potential of the CPE exponent, in which the additional specific adsorptions and the 2D phase restructuring at the electrode/electrolyte interface take place. On the other hand, for Au(pc) electrodes, the $E_{C'DL,min}$ almost coincides with the PME, and no order/disorder transition potential of the CPE exponent is observed. This highlights that complex ionic interactions alter the electrical and electrochemical conditions on Pt(pc) surfaces compared to Au(pc) electrodes due to more pronounced electrode/electrolyte interface processes, making the modeling of charge distribution conditions more straightforward for Au(pc).

Furthermore, all parameters increase with increasing electrolyte pH on the RHE scale in Figures 4C and D. The data are also presented on the standard hydrogen electrode (SHE) scale in Figure S8 to allow comparison with the reported PZTC by the CO displacement method.[39,61] For Pt(pc) electrodes within the selected pH range, the potential of $C'_{DL,min}$, close to PZTC, increases linearly on the RHE scale with a slope of 59 mV/pH but remains approximately constant on the SHE scale, excluding the Nernst potential shift, which is consistent with the findings reported for Pt(111).[61,65] Nonetheless, the potential of $C'_{DL,min}$ and PME shift positively for Au(pc) on both the RHE and SHE scales, with a similar trend observed by Desic et al.[47] The weak hydrogen adsorption that affects the intrinsic interfacial structure where the hydrogen reactions occur at the onset potential for Pt(pc) electrodes rather than for Au(pc) electrodes can be a possible explanation. Still, further investigations are required to gain a more detailed view of the ion concentration influence on the complex behavior of electrified interfaces of polycrystalline materials. Despite the complexity of the EDL nature of polycrystalline materials due to the mixed response of present crystal faces on the electrode's surface and influences such as grain boundaries, varying grain sizes, and lattice defects, their experimental investigation is of immense importance for the advancement in the application of electrocatalysts.

Conclusions

Considering the common application of polycrystalline Pt- and Au-based catalysts in industrial energy conversion devices, particularly in concentrated solutions, we explored the impact of electrolyte concentration on the C_{DL} for both polycrystalline electrodes using $HClO_4$ solutions with a pH range from 0 to 2 without adding buffer solutions. For both Pt(pc) and Au(pc) electrodes, the CVs reveal that the redox peaks shift positively with increasing electrolyte pH, a phenomenon closely related to the co-adsorption processes of ions and solvents, extending beyond the expected thermodynamic Nernst shift. Furthermore, the stronger hydrogen adsorption processes on Pt than on Au surfaces cause converse C_{DL} trends with different pH. The minimum C_{DL} values increase with an increase in higher concentrations (lower pHs) for Au(pc); however, the opposite trend is observed for Pt(pc), which the Stern model cannot quantitatively predict. Moreover, the EIS method can differentiate the adsorption processes due to different time constants, which leads to a more precise determination of the C_{DL} compared to cyclic voltammetry. Nevertheless, the cyclic voltammetry and EIS methods show the same trend for both electrodes. This can be due to a small amount of faster ion adsorption occurring on Pt(surface), resulting in the difficulty of extracting the pure C_{DL}, which needs further investigation by in-situ techniques and theoretical calculations of more complex electrode/electrolyte interfaces. Furthermore, measuring the CPE exponent and describing the frequency dispersion of the EDL as a function of the electrode potential by EIS allows the detection of a 2D phase transition (mainly between the adsorbate and water molecular layers) on Pt(pc) compared to Au(pc) electrodes. The positive linear trends with electrolyte pH

are found for PME, $E_{C'DL,min}$, and the transition potential of the CPE exponent (only Pt(pc)). Combining these essential parameters in one study offers a more comprehensive experimental assessment of the EDL at solid/liquid interfaces. This work provides a perspective on the EDL of polycrystalline electrodes in dependence on the electrolyte pH that serves as a first step towards a combined interpretation of different EDL parameters. However, only more experimental and theoretical research on polycrystalline electrodes with state-of-the-art techniques allows for more new insights that can lead to a complete understanding of the EDL processes.

Acknowledgements

This work has been supported by funding from TUM Innovation Network for Artificial Intelligence powered Multifunctional Material Design (ARTEMIS) and German Research Foundation (DFG) under Germany's excellence strategy – EXC 2089/1 – 390776260, Germany's excellence cluster "e-conversion". A. S. B. and P. M. S. are grateful for the funding by the Deutsche Forschungsgemeinschaft (DFG, German Research Foundation) – SFB 1625, project number 506711657, subproject C04.

Conflict of Interests

The authors declare no conflict of interest.

Data Availability Statement

The data that support the findings of this study are available from the corresponding author upon reasonable request.

Keywords: Electrical double layer · Platinum · Gold · Electrolyte pH · Double layer capacitance · Impedance spectroscopy

[1] R. Parsons, *Chem. Rev.* **1990**, *90*, 813–826.
[2] E. Lust, *Electrical Double Layers. Double Layers at Single-crystal and Polycrystalline Electrodes. In Encyclopedia of Electrochemistry*, A J. Bard (Ed.). Wiley-VCH Verlag, **2007**, DOI: 10.1002/9783527610426.bard010204.
[3] S. Xue, P. Chaudhary, M. R. Nouri, E. Gubanova, B. Garlyyev, V. Alexandrov, A. S. Bandarenka, *J. Am. Chem. Soc.* **2024**, *146*(6), 3883–3889.
[4] S. J. Shin, D. H. Kim, G. Bae, S. Ringe, H. Choi, H. K. Lim, C. H. Choi, H. Kim, *Nat. Comm.* **2022**, *13*, 174.
[5] J. P. Sabawa, A. S. Bandarenka, *Results Chem.* **2020**, *2*, 100078.
[6] C. Schütter, S. Pohlmann, A. Balducci, *Adv. Energy Mat.* **2019**, *9*, 1900334.
[7] A. H. B. Dourado, *Electrochem.* **2022**, *3*, 789–808.
[8] V. Locket, R. Sedev, J. Ralston, *J. Phys. Chem. C* **2008**, *112*, 7486–7495.
[9] S. A. Watzele, L. Katzenmeier, J. P. Sabawa, B. Garlyyev, A. S. Bandarenka, *Electrochim. Acta* **2021**, *391*, 138969.
[10] A. Alizadeh, M. Wang, *Electrophoresis* **2020**, *41*, 1067–1072.
[11] M. Ito, *Surf. Sci. Rep.* **2008**, *63*, 329–389.
[12] C. Leppin, A. Peschel, F. S. Meyer, A. Langhoff, D. Johannsmann, *Analyst* **2021**, *146*, 2160–2171.
[13] M. J. Bleda-Martínez, J. A. Maciá-Agulló, D. Lozano-Castelló, E. Morallón, D. Cazorla-Amorós, A. Linares-Solano, *Carbon* **2005**, *43*, 2677–2684.
[14] K. Ojha, N. Arulmozhi, D. Aranzales, M. T. M. Koper, *Angew. Chem.* **2020**, *132*, 721–725.
[15] A. Sadkowski, A. J. Motheo, R. S. Neves, *J. Electroanal. Chem.* **1998**, *455*, 107–119.
[16] P. Saha, I. V. Zenyuk, *J. Electrochem. Soc.* **2021**, *168*, 046511.
[17] P. Saha, I. V. Zenyuk, *J. Phys. Chem. C* **2021**, *125*, 19706–19715.
[18] B. L. Kuzin, D. I. Bronin, *Solid State Ion.* **2000**, *136–137*, 45–50.
[19] E. Gubanova, T. O. Schmidt, S. Watzele, V. Alexandrov, A. S. Bandarenka, *J. Phys. Chem. C* **2022**, *126*, 11414–11420.
[20] B. Garlyyev, S. Xue, S. Watzele, D. Scieszka, A. S. Bandarenka, *J. Phys. Chem. Lett.* **2018**, *9*, 1927–1930.
[21] S. Xue, B. Garlyyev, A. Auer, J. Kunze-Liebhäuser, A. S. Bandarenka, *J. Phys. Chem. C* **2020**, *124*, 12442–12447.
[22] M. M. Waegele, C. M. Gunathunge, J. Li, X. Li, *J. Chem. Phys.* **2019**, *151*, 160902.
[23] P. Sebastián, R. Martínez-Hincapié, V. Climent, J. M. Feliu, *Electrochim. Acta* **2017**, *228*, 667–676.
[24] R. W. Haid, X. Ding, T. K. Sarpey, A. S. Bandarenka, B. Garlyyev, *Curr. Opin. Electrochem.* **2022**, *32*, 100882.
[25] R. Rizo, E. Sitta, E. Herrero, V. Climent, J. M. Feliu, *Electrochim. Acta* **2015**, *162*, 138–145.
[26] A. Goyal, M. T. M. Koper, *Angew. Chem. Int. Ed.* **2021**, *60*, 13452–13462.
[27] T. K. Sarpey, E. Keles, E. L. Gubanova, A. S. Bandarenka, *Probing the electrified solid–liquid interfaces with laser-induced transient techniques. In Encyclopedia of Solid-Liquid Interfaces*, Wandelt, K., Bussetti, G., Eds., Elsevier: Amsterdam, **2024**, pp. 43–54.
[28] X. Ding, T. K. Sarpey, S. Hou, B. Garlyyev, L. Weijin, R. A. Fischer, A. S. Bandarenka, *ChemElectroChem* **2022**, *9*, e202101175.
[29] A. Ganassin, P. Sebastián, V. Climent, W. Schuhmann, A. S. Bandarenka, J. Feliu, *Sci. Rep.* **2017**, *7*, 1246.
[30] X. Ding, B. Garlyyev, S. A. Watzele, T. K. Sarpey, A. S. Bandarenka, *Chem. Eur. J.* **2021**, *27*, 10016–10020.
[31] J. Zheng, W. Sheng, Z. Zhuang, B. Xu, Y. Yan, *Sci. Adv.* **2016**, *2*, e1501602.
[32] D. Xing, D. Scieszka, S. Watzele, S. Xue, B. Garlyyev, R. W. Haid, A. S. Bandarenka, *ChemElectroChem* **2022**, *9*, e202101088.
[33] D. M. Morales, M. Risch, *JPhys Energy* **2021**, *3*, 034013.
[34] A. S. Bandarenka, *Analyst* **2013**, *138*, 5540–5554.
[35] V. Čolić, J. Tymoczko, A. Maljusch, A. Ganassin, W. Schuhmann, A. S. Bandarenka, *ChemElectroChem* **2014**, *2*, 143–149.
[36] A. S. Bondarenko, *Anal. Chim. Acta* **2012**, *743*, 41–50.
[37] R. Gisbert, G. García, M. T. M. Koper, *Electrochim. Acta* **2010**, *55*, 7961–7968.
[38] W. Sheng, Z. Zhuang, M. Gao, J. Zheng, J. G. Chen, Y. Yan, *Nat. Commun.* **2015**, *6*, 5848.
[39] N. Garcia-Araez, V. Climent, J. M. Feliu, *J. Electroanal. Chem.* **2010**, *649*, 69–82.
[40] J.-B. Le, Modeling Electrified Pt, *Jacs Au* **2021**, *1*, 569–577.
[41] I. T. McCrum, M. J. Janik, *J. Phys. Chem. C Nanomater. Interfaces* **2016**, *120*(1), 457–471.
[42] X. Chen, I. T. McCrum, K. A. Schwarz, M. J. Janik, M. T. M. Koper, *Angew. Chem. Int. Ed Engl.* **2017**, *56*(47), 15025–15029.
[43] P. Sebastián-Pascual, Y. Shao-Horn, M. Escudero-Escribano, *Curr. Opin. Electrochem.* **2022**, *32*, 100918.
[44] D. Pletcher, S. Sotiropoulos, *J. Chem. Soc. Faraday Trans* **1994**, *90*(24), 3663–3668.
[45] P. Xu, A. D. von Rueden, R. Schimmenti, M. Mavrikakis, J. Suntivich, *Nat. Mater.* **2023**, *22*(4), 503–510.
[46] C. H. Hamann, A. Hamnett, W. Vielstrich, *Electrochemistry*, 2nd, Completely Revised and Updated Edition, WILEY-VCH, **2007**.
[47] M. Desic, N. M. Popovic, M. M. D. Obradovic, L. M. Vracar, B. N. Grgur, *J. Serb. Chem. Soc.* **2005**, *70*(2), 231–242.
[48] J. Huang, *J. Chem. Theory Comput.* **2023**, *19*, 1003–1013.
[49] I. A. Bagotskaya, B. B. Damaskin, M. D. Levi, *J. Electroanal. Chem. Interfacial Electrochem.* **1980**, *115*(2), 189–209.
[50] P. Li, J. Huang, Y. Hu, S. Chen, *J. Phys. Chem. C Nanomater. Interfaces* **2021**, *125*(7), 3972–3979.
[51] J. Huang, *JACS Au* **2023**, *3*, 550–564.
[52] O. Gharbi, M. T. T. Tran, B. Tribollet, M. Turmine, V. Vivier, *Electrochim. Acta* **2020**, *343*, 136109.
[53] M. Schalenbach, Y. E. Durmus, H. Tempel, H. Kungl, R.-A. Eichel, *Phys. Chem. Chem. Phys.* **2021**, *23*, 21097–21105.
[54] M. D. Pohl, V. Colic, D. Scieszka, A. S. Bandarenka, *Phys. Chem. Chem. Phys.* **2016**, *18*, 10792–10799.
[55] X. Chen, I. T. McCrum, K. A. Schwarz, M. J. Janik, M. T. M. Koper, *Angew. Chem. Int. Ed Engl.* **2017**, *56*(47), 15025–15029.

[56] M. C. O. Monteiro, M. T. M. Koper, *Curr. Opin. Electrochem.* **2021**, *25*(100649), 100649.
[57] P. Li, Y. Jiao, J. Huang, S. Chen, *JACS Au* **2023**, *3*(10), 2640–2659.
[58] B. B. Berkes, G. Inzelt, W. Schuhmann, A. S. Bondarenko, *J. Phys. Chem. C* **2012**, *116*, 10995–11003.
[59] T. Pajkossy, T. Wandlowski, D. M. Kolb, *J. Electroanal. Chem. (Lausanne Switz)* **1996**, *414*(2), 209–220.
[60] J. Tymoczko, W. Schuhmann, A. S. Bandarenka, *Electrochem. Commun.* **2013**, *27*, 42–45.
[61] J. Tymoczko, V. Colic, A. S. Bandarenka, W. Schuhmann, *Surf. Sci.* **2015**, *631*, 81–87.
[62] A. Lasia, *J. Phys. Chem. Lett.* **2022**, *13*(2), 580–589.
[63] R. Martínez-Hincapié, P. Sebastián-Pascual, V. Climent, J. M. Feliu, *Russ. J. Electrochem.* **2017**, *53*, 227–236.
[64] R. Müller, J. Fuhrmann, M. Landstorfer, *J. Electrochem. Soc.* **2020**, *167*, 106512.
[65] N. L. Fröhlich, J. J. J. Eggebeen, M. T. M. Koper, *Electrochim. Acta* **2024**, *494*, 144456.

Manuscript received: October 20, 2024
Revised manuscript received: November 15, 2024
Version of record online: January 31, 2025